PROCEEDINGS OF SCIENCE

Search for $K^+ \to \pi^+ \nu\overline{\nu}$ at NA62

Jacopo Pinzino[*†]
CERN
E-mail: jacopo.pinzino@cern.ch

The decay $K^+ \to \pi^+ \nu\overline{\nu}$ has a very precisely predicted branching ratio ($\sim 8 \times 10^{-11}$) and it is one of the best candidates to reveal indirect effects of new physics. The NA62 experiment at CERN SPS is designed to measure the branching ratio of the $K^+ \to \pi^+ \nu\overline{\nu}$ with a decay-in-flight technique, novel for this channel. NA62 has taken data firstly in 2016 with the aim to reach the SM sensitivity. It has then collected 10 times more statistics in 2017 and a similar amount of data is expected from the 2018 run. The preliminary result on the full 2016 data set and the prospects for future developments are presented here.

XIV International Conference on Heavy Quarks and Leptons (HQL2018)
May 27- June 1, 2018
Yamagata Terrsa, Yamagata,Japan

[*]Speaker.

[†]On behalf of the NA62 Collaboration: R. Aliberti, F. Ambrosino, R. Ammendola, B. Angelucci, A. Antonelli, G. Anzivino, R. Arcidiacono, M. Barbanera, A. Biagioni, L. Bician, C. Biino, A. Bizzeti, T. Blazek, B. Bloch-Devaux, V. Bonaiuto, M. Boretto, M. Bragadireanu, D. Britton, F. Brizioli, M.B. Brunetti, D. Bryman, F. Bucci, T. Capussela, A. Ceccucci, P. Cenci, V. Cerny, C. Cerri, B. Checcucci, A. Conovaloff, P. Cooper, E. Cortina Gil, M. Corvino, F. Costantini, A. Cotta Ramusino, D. Coward, G. D'Agostini, J. Dainton, P. Dalpiaz, H. Danielsson, N. De Simone, D. Di Filippo, L. Di Lella, N. Doble, B. Dobrich, F. Duval, V. Duk, J. Engelfried, T. Enik, N. Estrada-Tristan, V. Falaleev, R. Fantechi, V. Fascianelli, L. Federici, S. Fedotov, A. Filippi, M. Fiorini, J. Fry, J. Fu, A. Fucci, L. Fulton, E. Gamberini, L. Gatignon, G. Georgiev, S. Ghinescu, A. Gianoli, M. Giorgi, S. Giudici, F. Gonnella, E. Goudzovski, C. Graham, R. Guida, E. Gushchin, F. Hahn, H. Heath, T. Husek, O. Hutanu, D. Hutchcroft, L. Iacobuzio, E. Iacopini, E. Imbergamo, B. Jenninger, K. Kampf, V. Kekelidze, S. Kholodenko, G. Khoriauli, A. Khotyantsev, A. Kleimenova, A. Korotkova, M. Koval, V. Kozhuharov, Z. Kucerova, Y. Kudenko, J. Kunze, V. Kurochka, V.Kurshetsov, G. Lanfranchi, G. Lamanna, G. Latino, P. Laycock, C. Lazzeroni, M. Lenti, G. Lehmann Miotto, E. Leonardi, P. Lichard, L. Litov, R. Lollini, D. Lomidze, A. Lonardo, P. Lubrano, M. Lupi, N. Lurkin, D. Madigozhin, I. Mannelli, G. Mannocchi, A. Mapelli, F. Marchetto, R. Marchevski, S. Martellotti, P. Massarotti, K. Massri, E. Maurice, M. Medvedeva, A. Mefodev, E. Menichetti, E. Migliore, E. Minucci, M. Mirra, M. Misheva, N. Molokanova, M. Moulson, S. Movchan, M. Napolitano, I. Neri, F. Newson, A. Norton, M. Noy, T. Numao, V. Obraztsov, A. Ostankov, S. Padolski, R. Page, V. Palladino, C. Parkinson, E. Pedreschi, M. Pepe, M. Perrin-Terrin, L. Peruzzo, P. Petrov, F. Petrucci, R. Piandani, M. Piccini, J. Pinzino, I. Polenkevich, L. Pontisso, Yu. Potrebenikov, D. Protopopescu, M. Raggi, A. Romano, P. Rubin, G. Ruggiero, V. Ryjov, A. Salamon, C. Santoni, G. Saracino, F. Sargeni, V. Semenov, A. Sergi, A. Shaikhiev, S. Shkarovskiy, D. Soldi, V. Sougonyaev, M. Sozzi, T. Spadaro, F. Spinella, A. Sturgess, J. Swallow, S. Trilov, P. Valente, B. Velghe, S. Venditti, P. Vicini, R. Volpe, M. Vormstein, H. Wahl, R. Wanke, B. Wrona, O. Yushchenko, M. Zamkovsky, A. Zinchenko.

PoS(HQL2018)027

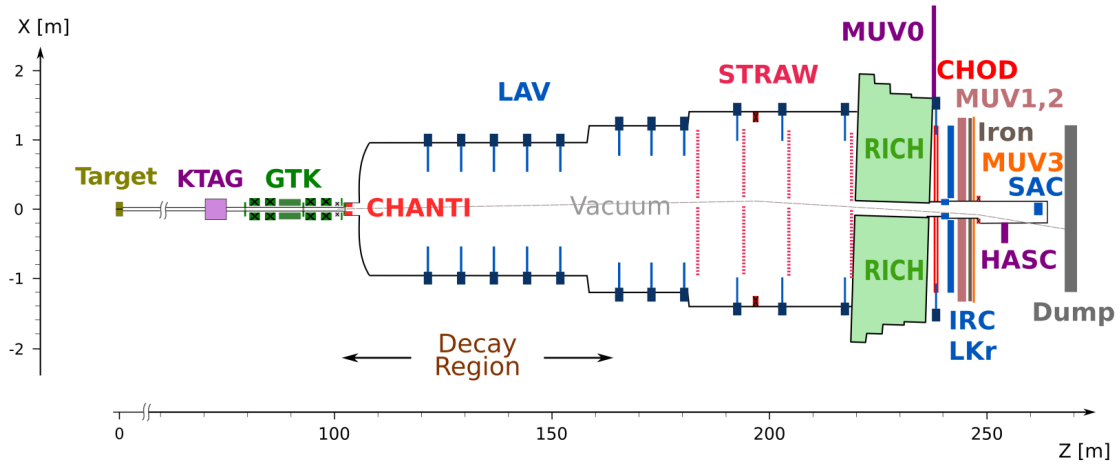

Figure 1: Schematic layout of the NA62 experiment in the xz plane

1. The $K^+ \to \pi^+ \nu\bar{\nu}$ decay in the Standard Model

The $K^+ \to \pi^+ \nu\bar{\nu}$ ($K_{\pi\nu\bar{\nu}}$) decay is a flavour changing neutral current process proceeding through W-box and electroweak Z-penguin diagrams. The process is ultra-rare because it is suppressed by the quadratic GIM mechanism and the Cabibbo-Kobayashi-Maskawa (CKM) matrix elements. The top-quark contribution is dominant and the $s \to d$ transition is described by short-distance quark dynamics, with a small charm quark contribution and long-distance corrections. This makes the $K_{\pi\nu\bar{\nu}}$ very clean theoretically and sensitive to physics beyond the Standard Model (SM), probing the highest mass scales among the rare meson decays [1, 2, 3, 4, 5, 6]. The SM prediction using elements of the CKM matrix extracted from tree-level processes [7, 8] is

$$BR(K^+ \to \pi\nu\bar{\nu}) = (8.4 \pm 1.0) \times 10^{-11}. \tag{1.1}$$

The knowledge of the external inputs (e.g. the knowledge of the CKM matrix parameters) dominates the uncertainties on the predictions. The most accurate measurement of this decay [9],

$$BR(K^+ \to \pi\nu\bar{\nu}) = (17.3^{+11.5}_{-10.5}) \times 10^{-11}, \tag{1.2}$$

was obtained by the E787 experiment and its upgrade E949 at BNL (from 1995 to 2002) using stopped kaons. The branching ratio is $\sim 1\ \sigma$ away from the SM prediction, but the measurement was based on only few events and the experimental uncertainties are large.

2. NA62 Experimental Setup

The NA62 experiment aims to improve the measurement of the $K_{\pi\nu\bar{\nu}}$ branching ratio reaching a precision of at least 10%. A sample of about 10^{13} kaon decays should be collected in a few years of data-taking using the 400 GeV/c primary Super-Proton-Synchrotron (SPS) proton beam. The primary beam hits a beryllium target to generate a secondary beam composed of π^+ (70%), p (23%) and K^+ (6%) with an average momentum of (75.0±0.8) GeV/c. A 100 m long beam line selects, collimates, focuses and transports charged particles to the evacuated fiducial decay volume.

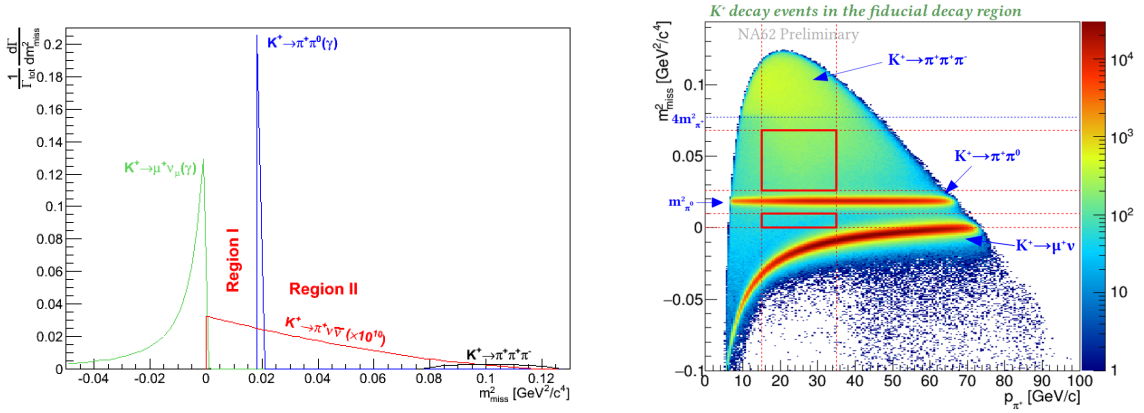

Figure 2: Left: m^2_{miss} shapes for signal and backgrounds of the main K^+ decay modes: the backgrounds are normalized according to their branching ratio; the signal is multiplied by a factor 10^{10}. Right: Distribution of m^2_{miss} as a function of track momentum for events selected on minimum bias data; The bands corresponding to $K^+ \to \pi^+\pi^0$ and $K^+ \to \mu^+\nu_\mu$ decays are clearly visible; the signal regions (red box) are drawn for reference.

A maximum of 10% of background contamination is required, necessitating a background rejection factor of the order of 10^{12}.

The K^+ in the beam is identified and timestamped by the KTAG, a nitrogen-filled differential Cherenkov detector. The momentum and directions of all beam particles are measured with the Gigatracker (GTK) composed of three silicon pixel stations of 6×3 cm^2 surface exposed to the full 750 MHz beam rate. The CHANTI detector, placed after the Gigatracker, tags hadronic beam-detector interactions in the last GTK station.

Downstream, the charged decay products are tracked by a magnetic straw chambers spectrometer. A dipole magnet between the second and third chamber is used to measure the momentum of the charged K^+ decay particles. A 17 m long RICH counter filled with neon gas is used to separate and to identify π^+, μ^+ and e^+. The time of charged particles is measured both with the RICH and with an array of scintillators (CHOD) located downstream of the RICH. Two hadronic calorimeters (MUV1 and MUV2) and a fast scintillator array (MUV3) provide further separation between π^+ and μ^+.

The most important source of background is the $K^+ \to \pi^+\pi^0$ decay, where the two photons from the π^0 are missed. A photon veto system is designed to reject these events. It is composed of a Large Angle Veto (LAV) detector made of 12 stations of lead-glass rings, a Liquid Krypton electromagnetic calorimeter (LKr) and two shashlik calorimeters (IRC, SAC), which hermetically cover all angles up to 50 mrad.

The NA62 experimental apparatus is shown in Figure 1 and its detailed description can be found in the NA62 beam and detector paper [10].

3. The $K^+ \to \pi^+ \nu\bar{\nu}$ analysis

The analysis of the complete 2016 data set is presented here, corresponding to a total number

of kaon decays in the fiducial decay region $N_K = 1.21(2) \times 10^{11}$. The $K^+ \to \pi^+ \nu\overline{\nu}$ signature is one track in the final state matched in time with one K^+ track upstream the decay region and nothing else, because the two neutrinos are undetectable. The main kinematic variable is $m^2_{miss} \equiv (p_K - p_{\pi^+})^2$, where p_K and p_{π^+} are the 4-momenta of the K^+ and π^+ respectively. The theoretical shape of the main K^+ background decay modes are compared to $K_{\pi\nu\overline{\nu}}$ in Figure 2-left.

The analysis is performed in two separate regions: Region 1 (R1) between the $K^+ \to \mu^+ \nu_\mu$ ($K_{\mu\nu}$) and $K^+ \to \pi^+\pi^0$ ($K_{\pi\pi}$) contributions and Region 2 (R2) between $K_{\pi\pi}$ and $K^+ \to \pi^+\pi^+\pi^-$ ($K_{\pi\pi\pi}$) contribution. The main backgrounds entering those regions are $K_{\mu\nu}$ and $K_{\pi\pi}$ decays through non-gaussian resolution and radiative tails; $K_{\pi\pi\pi}$ through non-gaussian resolution; $K^+ \to \pi^+\pi^- e^+ \nu_e$ (K_{e4}) and $K^+ \to l^+\pi^0\nu_l$ (K_{l3}) decays with neutrinos in the final state ($l = \mu, e$); upstream background consisting of K^+ decays upstream of the GTK3 station and inelastic beam-detector interactions. Each of the background processes requires different rejection procedure depending on its kinematics and type of charged particle in the final state.

The main requirements for the analysis are: excellent kinematic reconstruction to reduce kinematic tails; precise timing to reduce the kaon mis-tagging probability; no extra in-time activity in all of the electromagnetic calorimeters to suppress $\pi^0 \to \gamma\gamma$ decays (photon rejection); clear separation between $\pi/\mu/e$ tracks to suppress decays with μ^+ or e^+ in the final state (particle identification); and low multiplicity cuts in the downstream detectors to further suppress decays with multiple charged tracks in the final state.

Events with single track topology are selected using the downstream detectors STRAW, CHOD and RICH. The reconstructed track must have a matching pair of slabs in the CHOD and a reconstructed ring in the RICH, where the time is measured with 100 ps resolution. The downstream track is then associated to an in-time kaon in the KTAG detector. The K^+ track is reconstructed and time-stamped in the GTK detector. A kaon decay vertex is created at the intersection point of the GTK and STRAW tracks. The kaon decays within a 50 m fiducial region beginning 10 m downstream to the last GTK station (GTK3) are selected (Figure 2-right).

The π^+ tracks are identified by the calorimeters and the RICH counter providing 10^8 muon suppression for 64% π^+ efficiency. The performances are measured on kinematically selected $K_{\pi\pi}$ and $K_{\mu\nu}$ decays on control-trigger data.

Events passing the π^+ identification criteria are mainly $K_{\pi\pi}$ decays, which are further suppressed by rejecting in-time coincidences between the π^+ and energy deposits in the electromagnetic calorimeters LKr, LAVs, SAC, IRC. The resulting π^0 suppression is 3×10^{-8}, as measured from minimum bias and $K_{\pi\nu\overline{\nu}}$-trigger streams before and after γ rejection, respectively.

Signal region definitions are driven by the $m^2_{miss}(STRAW, GTK)$ resolution $\sigma(m^2_{miss}) = 1 \times 10^{-3}$ GeV$^2/c^4$. To protect against kinematic misreconstruction additional constraints are imposed on the $m^2_{miss}(RICH, GTK)$ computed by replacing the STRAW momentum with that measured by the RICH under a π^+ mass hypothesis and $m^2_{miss}(STRAW, Beam)$ computed by using nominal K^+ momentum. The total $K_{\pi\nu\overline{\nu}}$ acceptance after the complete selection and signal region definition is 4%, divided between R1(1%) and R2(3%).

The probability of the $K_{\mu\nu}(K_{\pi\pi})$ decays to enter the signal regions defined by the three m^2_{miss} is $3 \times 10^{-4}(1 \times 10^{-3})$. This kinematic suppression factor is used for the background estimation and is measured using $K_{\mu\nu}(K_{\pi\pi})$ decays selected with $\pi\nu\overline{\nu}$-like selection on a control-trigger data sample.

Source	δSES (10^{-10})
Random veto	± 0.17
Definition of $\pi^+\pi^0$ region	± 0.10
$A_{\pi\nu\nu}$	± 0.09
N_K	± 0.05
Trigger efficiency	± 0.04
Extra activity	± 0.02
Pileup simulation	± 0.02
Momentum spectrum	± 0.01
Total	± 0.24

Table 1: Sources of systematic uncertainties to single event sensitivity *SES*. See text for the definition of the various sources.

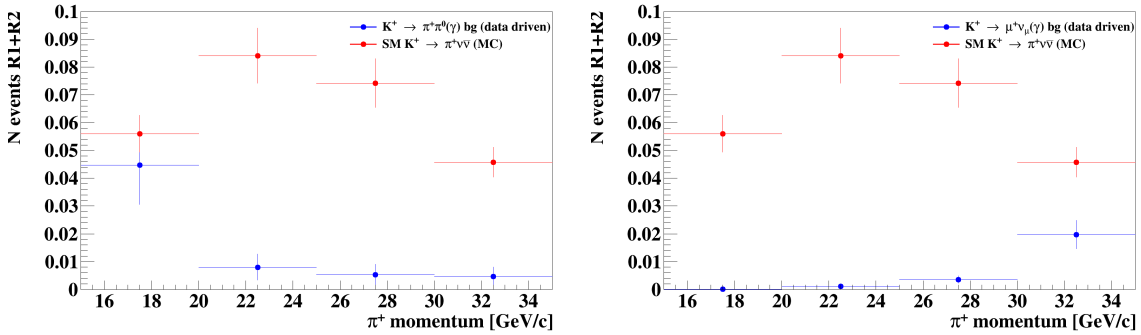

Figure 3: Left: Expected number of $K^+ \to \pi^+\pi^0(\gamma)$ background events in R1 and R2 in bins of P_{π^+} compared to the expected number of SM $K^+ \to \pi^+\nu\bar{\nu}$ events. Right: Same as left plot, but for the $K^+ \to \mu^+\nu_\mu(\gamma)$ background. Uncertainties on the background estimations are statistical only, while on expected signal are mostly systematic.

The single event sensitivity for a SM $K_{\pi\nu\bar{\nu}}$ decay is $SES = (3.15 \pm 0.01_{stat} \pm 0.24_{syst}) \times 10^{-10}$, dominated by systematic uncertainty. A summary of the systematic uncertainties on the *SES* is presented in Table 1. The uncertainty is dominated by: random veto losses induced by the π^0 rejection procedure; stability of the *SES* estimation when varying the $\pi^+\pi^0$ normalization region; simulation of the π^+ losses due to interactions in the detector material upstream of the hodoscopes.

The behaviour of the $K^+ \to \pi^+\pi^0(\gamma)$ and $K^+ \to \mu^+\nu_\mu(\gamma)$ background decays is shown in Figure 3 as a function of the P_{π^+} momentum and compared to the signal expectation. The $K_{\pi\pi(\gamma)}$ ($K_{\mu\nu}$) background is dominating at low(high) P_{π^+}.

The shape of the other background processes cannot be studied with the 2016 data set because of the limited statistics. A MC simulation of 400 million generated $K^+ \to \pi^+\pi^- e^+\nu_e$ (K_{e4}) decays is used to estimate the expected background. The simulation is validated on data using 5 independent samples. The precision of the K_{e4} background estimation is limited by the size of the MC sample. The upstream background is estimated using a data driven method. The method is statistically limited, reflected in the large uncertainty dominating the overall background estimation.

Process	Expected events in R1+R2
$K^+ \to \pi^+ \nu\bar{\nu}$ (SM)	$0.267 \pm 0.001_{stat} \pm 0.020_{syst} \pm 0.032_{ext}$
$K^+ \to \pi^+ \pi^0(\gamma)$ IB	$0.064 \pm 0.007_{stat} \pm 0.006_{syst}$
$K^+ \to \mu^+ \nu(\gamma)$ IB	$0.020 \pm 0.003_{stat} \pm 0.003_{syst}$
$K^+ \to \pi^+ \pi^- e^+ \nu$	$0.018^{+0.024}_{-0.017}\|_{stat} \pm 0.009_{syst}$
$K^+ \to \pi^+ \pi^+ \pi^-$	$0.002 \pm 0.001_{stat} \pm 0.002_{syst}$
Upstream Background	$0.050^{+0.090}_{-0.030}\|_{stat}$
Total Background	$0.15 \pm 0.09_{stat} \pm 0.01_{syst}$

Table 2: Summary of the expected number of signal and background events in R1 and R2 after the $K_{\pi\nu\bar{\nu}}$ analysis is applied on the complete 2016 data set.

4. Results

One event is found in R2 after un-blinding the signal regions. The $K_{\pi\nu\bar{\nu}}$ candidate event (Figure 4-left) has 15.3 GeV/c momentum and is perfectly consistent with a π^+ track in the RICH detector (Figure 4-right).

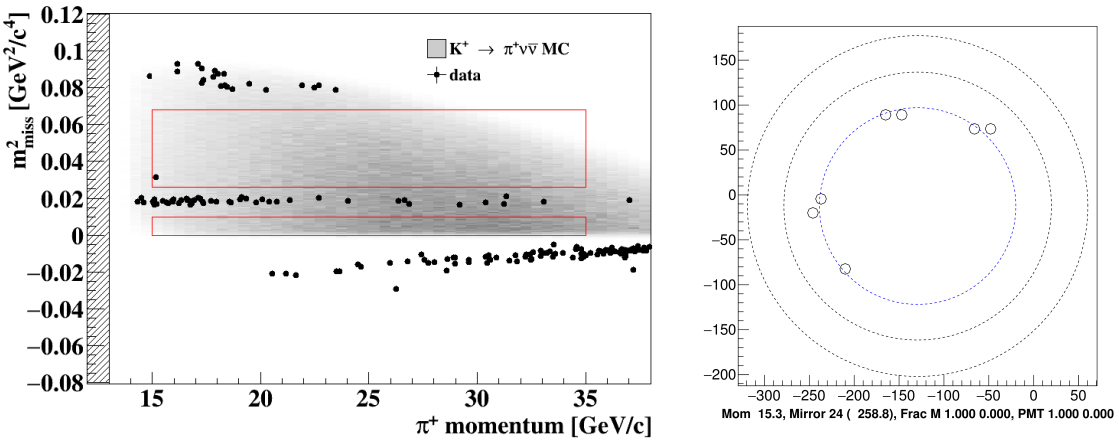

Figure 4: Left: m^2_{miss} as a function of P_{π^+} (dots) after the complete $K^+ \to \pi^+ \nu\bar{\nu}$ selection is applied, but the cuts on m^2_{miss} and P_{π^+}. The grey area corresponds to the distribution of $K^+ \to \pi^+ \nu\bar{\nu}$ MC events. The red lines correspond to the two signal regions. The event observed in R2 is shown. Right: Position of the hits in the RICH forming the ring associated to the π^+ track in the observed event in R2, given by the RICH event display. The circles illustrate the positron, muon and pion hypothesis, showing a perfect agreement with the pion hypothesis (the innermost ring).

Upper limits on the branching ratio of the $K^+ \to \pi^+ \nu\bar{\nu}$ decay are obtained using the CL$_s$ method [11]:

$$BR(K^+ \to \pi^+ \nu\bar{\nu}) < 14 \times 10^{-10} \text{ @ 95\% CL observed limit}$$
$$BR(K^+ \to \pi^+ \nu\bar{\nu}) < 10 \times 10^{-10} \text{ @ 95\% CL expected limit.}$$

Alternatively the Rolke-Lopez method [12] is used, assuming a Poisson process in the presence of background with a gaussian uncertainty. The results are in agreement with the CL_s treatment.

A measurement of the branching ratio at 68% CL is also computed after subtracting the expected background

$$BR(K^+ \to \pi^+ \nu\bar{\nu}) = 2.8^{+4.4}_{-2.3} \times 10^{-10} \text{ @ } 68\% \text{ CL.}$$

No statistically significant signal observation can be claimed, therefore the branching ratio is shown only for comparison with the result obtained by the BNL E949 collaboration $BR(K^+ \to \pi^+ \nu\bar{\nu}) = 1.73^{+1.15}_{-1.05} \times 10^{-10}$ @ 68% CL [9] and with the Standard Model prediction $BR(K^+ \to \pi^+ \nu\bar{\nu}) = (0.84 \pm 0.10) \times 10^{-10}$. Our result is in agreement with both the SM prediction and previous measurements.

The analysis of the 2016 data set proves that the decay-in-flight technique of NA62 to study $K^+ \to \pi^+ \nu\bar{\nu}$ works. The $K^+ \to \pi^+ \nu\bar{\nu}$ analysis of the 2017 data is ongoing. Improvements at both hardware and analysis level are foreseen to reduce the background and to increase the signal efficiency. Considering the statistics collected in 2017 and expected in 2018, NA62 should observe about 20 SM $K^+ \to \pi^+ \nu\bar{\nu}$ events with the complete data set.

References

[1] M. Blanke, A. J. Buras, B. Duling, K. Gemmler and S. Gori, "Rare K and B Decays in a Warped Extra Dimension with Custodial Protection," JHEP **0903** (2009) 108 doi:10.1088/1126-6708/2009/03/108 [arXiv:0812.3803 [hep-ph]].

[2] A. J. Buras, D. Buttazzo and R. Knegjens, "$K \to \pi\nu\bar{\nu}$ and ε'/ε in simplified new physics models," JHEP **1511** (2015) 166 doi:10.1007/JHEP11(2015)166 [arXiv:1507.08672 [hep-ph]].

[3] T. Blažek and P. Maták, "Left-left squark mixing, $K+ \to \pi^+ \nu\bar{\nu}$ and minimal supersymmetry with large tanβ," Int. J. Mod. Phys. A **29** (2014) no.27, 1450162 doi:10.1142/S0217751X14501620 [arXiv:1410.0055 [hep-ph]].

[4] G. Isidori, F. Mescia, P. Paradisi, C. Smith and S. Trine, "Exploring the flavour structure of the MSSM with rare K decays," JHEP **0608** (2006) 064 doi:10.1088/1126-6708/2006/08/064 [hep-ph/0604074].

[5] M. Blanke, A. J. Buras and S. Recksiegel, "Quark flavour observables in the Littlest Higgs model with T-parity after LHC Run 1," Eur. Phys. J. C **76** (2016) no.4, 182 doi:10.1140/epjc/s10052-016-4019-7 [arXiv:1507.06316 [hep-ph]].

[6] M. Bordone, D. Buttazzo, G. Isidori and J. Monnard, "Probing Lepton Flavour Universality with $K \to \pi\nu\bar{\nu}$ decays," Eur. Phys. J. C **77** (2017) no.9, 618 doi:10.1140/epjc/s10052-017-5202-1 [arXiv:1705.10729 [hep-ph]].

[7] A. J. Buras, D. Buttazzo, J. Girrbach-Noe and R. Knegjens, "$K^+ \to \pi^+ \nu\bar{\nu}$ and $K_L \to \pi^0 \nu\bar{\nu}$ in the Standard Model: status and perspectives," JHEP **1511** (2015) 033 doi:10.1007/JHEP11(2015)033 [arXiv:1503.02693 [hep-ph]].

[8] J. Brod, M. Gorbahn and E. Stamou, "Two-Loop Electroweak Corrections for the $K \to \pi\nu\bar{\nu}$ Decays," Phys. Rev. D **83** (2011) 034030 doi:10.1103/PhysRevD.83.034030 [arXiv:1009.0947 [hep-ph]].

[9] A. V. Artamonov *et al.* [BNL-E949 Collaboration], "Study of the decay $K^+ \to \pi^+ \nu\bar{\nu}$ in the momentum region $140 < P_\pi < 199$ MeV/c," Phys. Rev. D **79** (2009) 092004 doi:10.1103/PhysRevD.79.092004 [arXiv:0903.0030 [hep-ex]].

[10] E. Cortina Gil *et al.* [NA62 Collaboration], "The Beam and detector of the NA62 experiment at CERN," JINST **12** (2017) no.05, P05025 doi:10.1088/1748-0221/12/05/P05025 [arXiv:1703.08501 [physics.ins-det]].

[11] A. L. Read, "Presentation of search results: The CL(s) technique," J. Phys. G **28** (2002) 2693. doi:10.1088/0954-3899/28/10/313

[12] W. A. Rolke and A. M. Lopez, "Correcting the minimization bias in searches for small signals," Nucl. Instrum. Meth. A **503** (2003) 617 doi:10.1016/S0168-9002(03)00428-5 [hep-ph/0206139].